Pharm Res (2014) 31:1632–1643
DOI 10.1007/s11095-013-1266-2

RESEARCH PAPER

Co-delivery of Dexamethasone and Green Tea Polyphenols Using Electrospun Ultrafine Fibers for Effective Treatment of Keloid

Jinrong Li • Rong Fu • Long Li • Guang Yang • Shan Ding • Zhendong Zhong • Shaobing Zhou

Received: 4 September 2013 / Accepted: 9 December 2013 / Published online: 7 January 2014

ABSTRACT

Purpose The electrospun polymer ultrafine fiber meshes wereused to co-deliver dexamethasone (DEX) and green tea polyphenols (GTP) in order to acquire a suitable balance between effective treament of keloid and safety to the skin.

Methods This co-delivery system was prepared with a simple electrospinning technology. Keloid model was established on the back of athymic nude mice with the human keloid tissues and the formulated fiber meshes were applied onto keloids for an *in vivo* evaluation on their therapeutic effects.

Results Unlike other therapeutic formulations, these fiber meshes as a new surgical dressing possess multiple useful functions, including the capabilities of maintaining a moist environment, resisting bacterial infection and controlling the drug release. Hydrophobic DEX molecules inside the fiber meshes can be released successfully from the channels formed by the early release of the hydrophilic GTP molecules and then transported across the skin. A distinctive result acquired from histological analysis shows that after 3-month treatment, the DEX/GTP-loaded fiber meshes significantly induce the degradation of collagen fibers in keloid on the back of nude mice compared to the traditional treatment.

Conclusion The dressing formulation based on nanofibers provides a promising platform for the treatment of keloid.

KEY WORDS Biodegradable · Drug delivery · Electrospinning · Polymer · Ultrafine

INTRODUCTION

Keloids are fibroproliferative lesions that occur at areas of cutaneous injury but do not regress and grow continuously beyond the original margins of the scars (1–3). They are benign but often cause pain, tenderness, pruritus, and paresthesias, in addition to aesthetically malignant. Although keloid remains a major healthcare problem for almost all countries, its management is still one of the most frustrating clinical problems in plastic and reconstructive surgery. In the past decades, various treatments were emerged, including intralesional steroid injection, surgical excision, cryotherapy, laser therapy, radiation therapy and the application of silicon gel sheeting (4), and acquired some therapeutic effects. However, keloids often recur or even become worse after these treatments (5–9).

As there is still no ideal treatment for keloid, more and more researchers have been dedicated to seeking the effective treatments for keloids. The transdermal therapy represents an

Electronic supplementary material The online version of this article (doi:10.1007/s11095-013-1266-2) contains supplementary material, which is available to authorized users.

L. Li • G. Yang • S. Zhou (✉)
Key Laboratory of Advanced Technologies of Materials
Ministry of Education, School of Materials Science & Engineering
Southwest Jiaotong University
Chengdu 610031, People's Republic of China
e-mail: shaobingzhou@hotmail.com; shaobingzhou@swjtu.edu.cn

J. Li • S. Ding • S. Zhou
School of Life Science and Engineering, Southwest Jiaotong University
Chengdu 610031, People's Republic of China

R. Fu • Z. Zhong
Plastic Surgery Department
Sichuan Academy of Medical Sciences & Sichuan Provincial People's Hospital
Chengdu 610212, People's Republic of China

attractive alternative ascribed to the existence of no pain and convenience in drug administration (10). More recently, drugs-entrapped electrospun polymer fibers have been fabricated as a dressing formulation to control the drug release (11–14). Electrospinning, a promising and versatile processing technique which utilizes electrical forces to produce polymer fibers using polymer solutions, has been developed in recent years. The resultant electrospun fiber meshes possess a high surface area to volume ratio and highly interconnected pores among fibers, manifesting a great potential for wound dressings for dermal therapy including keloids (15–19).

Dexamethasone (DEX) has been demonstrated to suppress fibroblast proliferation (20), and therefore has been proposed to be a therapeutic agent in clinic treatment of keloid via transdermal delivery, especially by intralesional injection. However, the intralesional injection of DEX often brings many side effects such as many pains for patients due to its strong hydrophobicity. Hence, the encapsulation of DEX into polymer matrix with the ability of controlled drug delivery such as the electrospun fibers represents a good approach to solve this problem. Green tea polyphenols (GTP), the naturally biologically active substances from tea, possess high hydrophilicity and many functions including antioxidant properties, and antibacterial and antiviral effects (21–23). Here, we anticipate that co-encapsulation of GTP with DEX into electrospun fibers would improve the hydrophilicity of the resultant drug-loaded fiber meshes and endow an antibacterial activity.

To date, it is still a challenging task to control the dose of drug efficiently penetrating into skin in the transdermal administration. In this study, we develop DEX/GTP-loaded electrospun biodegradable poly(lactic-co-glycolic acid) (PLGA) ultrafine fiber meshes as a dressing formulation for keloid treatment. The delivery route of drug across skin is schematically illustrated in Fig. 1. Hydrophilic GTP molecules are firstly diffused out from the fiber matrix and consequently some channels are formed. Later, hydrophobic DEX molecules inside the fiber meshes are released successfully from these channels, and then transported across the skin involving the mechanism of transdermal delivery. These molecules can exert the best therapeutic function after they penetrate into the three-layer structure (stratum corneum, epidermis and dermis) of the skin. The dual drug-loaded electrospun fiber meshes are further evaluated through their inhibition on keloid fibroblasts *in vitro* and keloids *in vivo*.

MATERIALS AND METHODS

Materials

PLGA with D, L-lactide and glycolide weight ratio of 70/30 was synthesized by ring-opening polymerization as previous report (24). Its weight-average molecular weight (Mw) determined by gel permeation chromatography (GPC; Waters 2695 and 2414) was about 100 kDa. Silicone scar sheet was from Shanghai Dong Yue Medical Health Products Co., Ltd. Dexamethasone (DEX) was purchased from Sigma-Aldrich. Green tea polyphenols (GTP) was kindly provided by Prof. X.D. Li in Sichuan University (China). All other chemicals and solvents were purchased from Chengdu Kelong Chemical Reagent Factory with reagent grade or better.

Fabricating of Electrospun Fibers

A 25% (*w/v*) PLGA solution was prepared using a mixture of acetone and N,N-dimethyl formamide (DMF) with a volume ratio of 3:1, in which both DEX at a concentration of 15% by weight of PLGA and GTP with a series of concentrations of

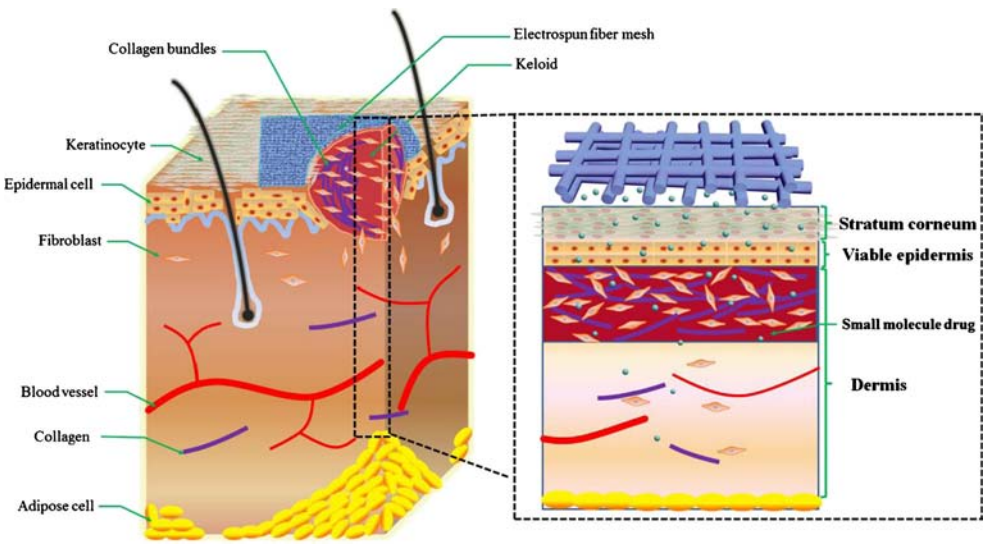

Fig. 1 Schematic representation of a cross section through skin by the way of transdermal delivery. Stratum corneum, located on the outer surface of the skin, is a non-living layer of keratin-filled cells surrounded by a lipid-rich extracellular matrix that provides the primary barrier to drug delivery into skin. The epidermis below is a viable tissue devoid of blood vessels. Just below the dermal-epidermal junction, the dermis contains capillary loops that can take up transdermally administered drugs for systemic distribution.

5%, 10%, and 15% by weight of PLGA are dissolved. The electrospinning process was performed at room temperature (22°C) with a humidity value between 50 and 70% (25). A voltage of 23 kV, a 23G stainless steel needle and a 30×40 cm ground collector were used and the needle tip-to-ground collector distance of 18 cm and a flow rate of 0.5 mL/h were defined as optimized processing conditions for electrospinning. The collected fiber meshes were dried under vacuum at room temperature for 3 days to completely remove solvent residue and then stored at 4°C. Herein, the so-called DEX/PLGA, DEX/GTP5/PLGA, DEX/GTP10/PLGA, DEX/GTP15/PLGA correspond to the PLGA fiber meshes with DEX loading of 15%, and GTP loading of 0%, 5%,10%,15%, respectively.

Characterization

The electrospun fibers were gold-coated using sputter coating to observe the surface topographies by SEM (FEI, Quanta 200, Philips, Netherlands). Micrographs were recorded at 20.0 kV with magnifications ranging from 1000 to 5000 times. Micrographs from the SEM analysis were digitized and analyzed with Image-Pro plus 6.0 to determine the average diameter and its distribution. The water contact angle (WCA) was measured at room temperature using a sessile drop method at room temperature with the contact angle equipment (DSA 100, KRUSS, Germany). The porosity of PLGA fiber meshes was calculated as described previously according to the following equation: Porosity = $(1- \rho/\rho_0)\times 100\%$, where ρ is the density of electrospun meshes and ρ_0 is the density of bulk polymer (26). Tensile mechanical properties of electrospun fiber meshes were performed using a universal test machine (Instron 5567, Instron Co., Masschusetts) at room temperature (22°C).

In Vitro Degradation

Preweighed electrospun PLGA fibers were placed in individual test tubes containing 40.0 mL of phosphate buffered saline (PBS) at pH 7.4. The tubes were kept in a thermostated shaking air bath that was maintained at 37°C under 120 cycles/min. The degradation lasted for 12 weeks. Every 2 weeks, triplicate specimens for each fiber mesh were retrieved from the tubes, rinsed several times with pure water, and kept in the 40 mL distilled water overnight to remove residual buffer salts completely, then dried to constant weight in a vacuum desiccator. The degree of degradation was estimated from the changes of surface morphology observed with SEM, mass loss determined gravimetrically by comparing the dry weight remaining at a specific time with the initial weight and the reduction of molecular weight of fiber matrix determined using GPC.

In Vitro Drug Release

The drug release profile from the electrospun fibers was studied as follows. The fiber meshes with weight of 50 mg were placed into individual test tubes containing 40.0 mL of PBS at pH 7.4 and incubated in a same air bath as mentioned in degradation test. At predetermined intervals, 3 mL of release medium was taken out and the same volume of fresh PBS was added back to the test tube. The amount of drug released at various times, up to 600 h, was determined using UV–vis spectrophotometry (Shimadzu UV-2551, Japan) at 242 nm for DEX and 275 nm for GTP by the aid of the calibration curves of each drug in the same release medium. These experiments were done in triplicate.

Antibacterial Activity

The electrospun meshes were microbiologically evaluated for antibacterial activity against the Gram-negative microorganism *Escherichia coli* (ATCC 25922). The assessment was investigated based on the method of disc agar diffusion. The medium surface was inoculated with a suspension of 24-h cell culture of *E. coli* (1×10^3cells/mL). All the meshes were trimmed into circular discs with a diameter of 15 mm and placed on the top of the agar plate. After that, the plates were incubated at 37°C for 24 h, after which the zones of inhibition around each disc were measured using Image-Pro plus 6.0, based on five measurements.

In Vitro Cytotoxicity Analysis

Firstly, PLGA fiber meshes were cut into small round pieces with areas of approximately 1.5 cm^2, and sterilized with ultraviolet irradiation through UV lamps. Then the fiber meshes were placed in 24- well tissue culture plate and tissue culture plate (TCP) was acted as control. Finally the meshes were immersed in fetal calf serum for 30 min prior to cell seeding. NIH 3 T3 fibroblasts were grown Dulbecco's Modified Eagle's Medium-high glucose (DMEM-LG, Hyclone) with 10% calf serum and 1% penicillin–streptomycin (Sigma). Cell suspension was pipetted directly into the wells with an initial seeding density of 2×10^4 cells/well, and maintained at 37°C in an atmosphere of 5% CO_2. The cell proliferation on the surface of fiber meshes was determined by means of the Alamar blue assay as specified by the manufacturer (Biosource, Nivelles, Belgium). In brief, at 1, 3, 5 and 7 days post cell seeding, culture medium was replaced with the working Alamar blue solution (10% Alamar blue, 80% media 199, Gibcos, and 10% FBS; V/V). After that, 200 μL samples of the supernatant from each well were collected and read at 570 nm(excitation)/600 nm(emission) in a ELISA microplate reader (Molecular Devices, Sunnyvale, CA). Results are

defined as mean±standard deviation, and each sample was performed in triplicate. Cells that cultured on PLGA, DEX/PLGA, DEX/GTP15/PLGA fiber meshes were analyzed by SEM (FEI, Quanta 200, Philips, Netherlands) at 3 and 7 days after seeding to characterize cell morphology, spreading, elongation, and growth on the surfaces of the fiber meshes. For SEM observation, the samples were washed twice with PBS and fixed with 2.5% glutaraldehyde overnight at 4°C. After that, the specimens were further dehydrated through a series of graded alcohol solutions and then let to dry overnight. The dry cellular meshes were finally sputter coated with palladium and observed under the SEM at an accelerating voltage of 20.0 kV.

In Vitro Inhibitory Effect of Keloid Fibroblasts

The cell suppression of drug-loaded PLGA fiber meshes were demonstrated using human keloid fibroblasts (hKFs). hKFs were isolated and characterized according to the classic tissue culture method. In brief, Keloid tissues derived from patients approving in advance undergoing keloid excision during surgery were collected aseptically in a tube containing DMEM-high glucose. The skin specimens were washed thrice with phosphate-buffered saline solution (PBS) and were cut into approximately 2-mm squares. The keloid fragments were inoculated into 6-well tissue culture plates, covered with 0.5 ml of FBS and supplied high DMEM with 10% fetal calf serum and 1% penicillin–streptomycin. Finally the 6-well tissue culture plates were incubated at 37°C in a humidified 5% CO_2 atmosphere. To maintain the tissue fragments adhere to the well, any observation and overturn were not done in the following 3 days. After confluence, cells were subcultured by treatment with trypsin. Cultured keloid fibroblasts of less than 15 generations were used for our experiments. The protocol of the study was approved by Academy of Medical Sciences & Sichuan Provincial People's Hospital. The keloid fibroblast cell inhibition of fiber meshes was also evaluated at time points of 1, 3, 5 and 7 days by means of the Alamar blue assay as described above. The cell morphology and distribution of samples were determined by staining of 1 μM calcein AM (Sigma America), and then observed by fluorescence microscopy (DMIL, Leica, Germany).

Establishment of Keloid Model

The keloid model was established in the subcutaneous tissue by transplanting human keloid tissues (27). Athymic nude mice (nu/nu), obtained from Slack laboratory animals Co, Ltd, Shanghai, Chinese Academy of Sciences, at the age of 3 to 5 weeks, were used in the experiment. They were kept in presterilized cages alone, and placed in a laminar flow sterile bench. Human keloid tissues were obtained from surgical operations as excess material, and kept under sterile conditions until used for implantation. The mice were anesthetized with sodium pentobarbital at a level of 50 mg/kg of body. In general, a 4 mm×4 mm×3 mm section of keloid was de-epithelialized and inserted through a 1 cm incision into a subcutaneous pouch on both sides of the back. The incision was closed with wound clips and the area was daubed with erythromycin. All procedure was carried out under aseptic conditions. The animal with no dressing was returned to an individual cage. The volume change of keloid after implanted in the nude mice was measured using micrometer caliper after establishment for 1~10 weeks, and calculated by measuring two dimensions and using the equation: Volume (mm^3)=$a \times b^2 \times 0.5$, where a and b are the longest and the shortest diameter, respectively (28).

Treatment of Keloid

When the implanted keloid reached a stable volume after 8 weeks, treatments were carried out. 20 mice were assigned to a control group and three experimental groups of 5 mice each. Fiber meshes were sterilized by UV lamps for 3 h in advance and soaked in physiological saline before treatment. The keloids were covered with PLGA, DEX/PLGA, DEX/GTP10/PLGA fiber meshes on one side, respectively, and the other side was treated with silicon gel sheeting as the positive control. All materials were sutured by wound clips, and daubed with erythromycin. Antiseptic gauze was covered on the fiber meshes and silicon gel sheeting to fix them. Fiber meshes dressings were wetted through directly dropping saline every other day. After treated with fiber meshes and silicone scar sheet, the volume of the keloid was also measured from 1 to 14 weeks and calculated as described above.

Histological Evaluation

After 14 weeks operation, the keloid tissues of five mice were obtained and fixed routinely by paraffin-embedded, sectioned and stained with hematoxylin and eosin (H&E) and Masson's trichrome staining. The histological slices obtained were observed by optical microscopy.

Statistics Analysis

The experiments values were expressed as means ± standard deviation (SD). Statistically significant differences were determined by one way analysis of variance (ANOVA). A probability value (p) of less than 0.05 was considered to be statistically significant.

RESULTS AND DISCUSSION

Characterization of Electrospun DEX/GTP-Loaded PLGA Fiber Meshes

Morphologies, sizes and distributions of fibers were examined using a scanning electron microscope (SEM). As shown in Fig. 2, the surface morphologies of all the resultant fiber meshes were smooth, and all the fibers with an average diameter of 780 nm had an uniform appearance in diameter, suggesting that the introducing of DEX/GTP into polymer matrix almost had no effect on fiber topographic features. From the SEM images, we could also find many interconnected pores with a high porosity of 90%±5% among these fibers, which would be very helpful to allow the interchange of gas between the interior tissue and the surrounding air, and the penetration of water across the meshes into skin (29). Figure S1 displays the mechanical properties such as young's modulus, maximum tensile strength (ε_{max}) and elongation at break for pure PLGA, PLGA fiber meshes loaded with DEX content of 15%, and GTP content of 0%, 5%,10%,15%, respectively. The maximum tensile strength (ε_{max}) maintained a slight increase from 1.7 MPa for PLGA to 1.9 MPa for DEX/GTP15/PLGA while the elongation at break emerged a sharp reduction from 114.48% for PLGA to 62.98% for DEX/PLGA, 55.18% for DEX/GTP5/PLGA, 48.11% for DEX/GTP10/PLGA and 32.43% for DEX/GTP15/PLGA with the increase of drug content in PLGA matrix, indicating that introduction of drug into the polymer matrix influenced the mechanical properties of fiber meshes as reported previously (30,31). However, for all these fiber meshes, the mechanical strength is enough to meet the requirement of skin tissue engineering (32).

In Vitro Degradation and Drug Release

The *in vitro* degradation of fiber matrix and the release of DEX and GTP from the electrospun fiber meshes were performed. As shown in Fig. 3a, after 12 weeks of degradation, all of the electrospun fiber meshes still remained their fibrous structure, and DEX/GTP15/PLGA fiber meshes were obviously swollen and broken down compared with other meshes, suggesting that the macromolecular chains might be cleaved because of the hydrolysis. Figure 3b and c show the gravimetric evaluation and molecular weight loss of the electrospun fiber meshes during incubation, respectively. The mass of the fiber meshes was decreased continuously *versus* incubation time and the rate of loss was elevated along with the increase of the hydrophilic drug (GTP) loaded into fiber matrix. The loss of molecular weight was also consistent with the loss of mass. Since previous reports have demonstrated that the surface hydrophilicity and hydrophobicity of the category of polyester polymer carrier play an important role in influencing degradation patterns due to the hydrolysis of ester bonds (33,34), we further characterized the surface hydrophilicity of PLGA fibers by measuring the water contact angle (WCA). As displayed in Fig. 3a, the WCAs of both pure PLGA and DEX/PLGA fiber meshes were at about 125°, suggesting that the addition of DEX did not affect the hydrophobicity of PLGA matrix. However, the WCA of GTP-loaded PLGA fiber meshes was decreased sharply from 101±4.1° to 0° along with the increase of the amount of GTP in fiber matrix, indicating that the natural hydrophilicity of GTP has greatly improved the hydrophilicity of PLGA fiber meshes as designed. Also, this modification is very important for keeping a moist environment for our following investigations including the controlled drug release *in vitro* and the treatment of keloid in nude mice.

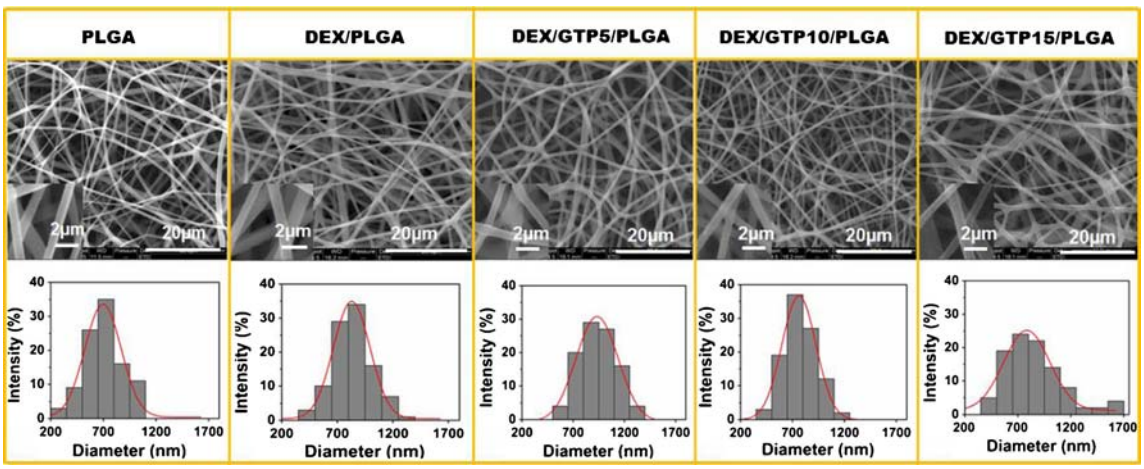

Fig. 2 Scanning electron microscopy images of PLGA, DEX/PLGA, DEX/GTP5/PLGA, DEX/GTP10/PLGA, DEX/GTP15/PLGA fiber meshes and their diameter distribution histograms.

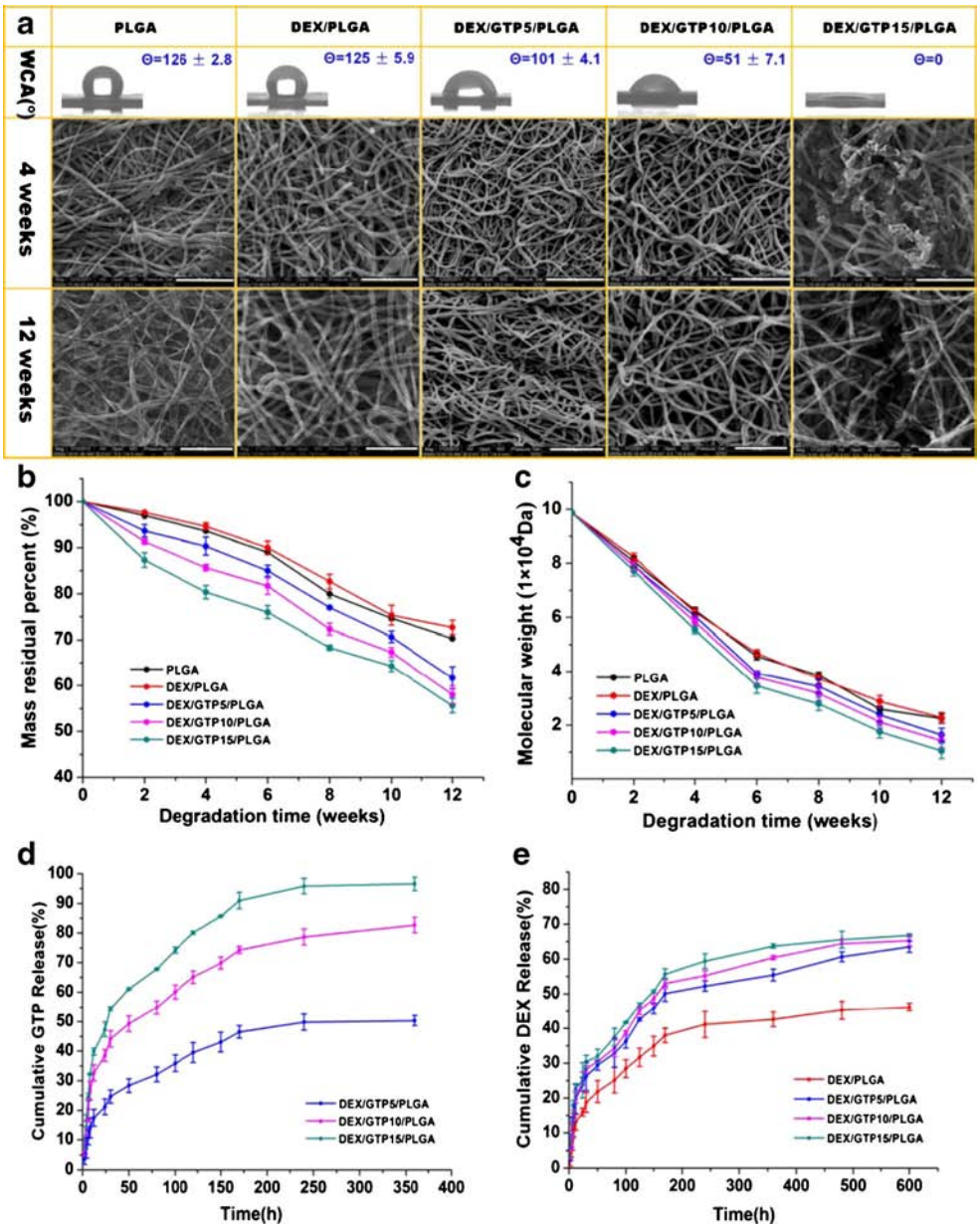

Fig. 3 *In vitro* degradation and drug release profiles of electrospun fiber meshes for PLGA, DEX/PLGA, DEX/GTP5/PLGA, DEX/GTP10/PLGA, DEX/GTP15/PLGA in PBS (pH 7.4) at 37°C. (**a**, **b**, **c**, **d** and **e**) Water contact angle (WCA) and selected scanning electron microscopy images (all the scale bars mean 20.0 μm), the mass residual percent, the reduction of molecular weight (Mw), the release profiles of dexamethasone (DEX) and green tea polyphenols (GTP) against incubation time, respectively.

Figure 3d and e show the release profiles of GTP and DEX from the electrospun meshes, respectively. A typical biphasic pattern was observed for the drug release from all of fiber meshes., Both drugs were released in a burst in the original phase and then stably in the following period. Within 600 h of incubation, only 45% of GTP was released from the meshes loaded with the lowest dose of GTP, while the cumulative release reached to 98% when the highest dose of GTP was loaded (Fig. 3d), indicating that the release behavior of GTP could be controlled by adjusting the ratio of polymer to hydrophilic drug. Interestingly, in 25 days experiment the release speed of hydrophobic DEX was also increased against the rate of hydrophilic GTP from fiber matrix (Fig. 3e), suggesting that these hydrophobic DEX molecules inside the fiber meshes could be released successfully via the channels formed by the fast release of hydrophilic GTP molecules. Figure S2 shows two mechanisms mainly involved in the release of DEX and GTP: diffusion of drug molecules and degradation of polymer matrix in the final period (35,36). In the original period, H_2O molecules in PBS firstly penetrated into fiber matrix which resulted in the diffusion of hydrophilic GTP molecules into PBS; The channels were thus formed in the fiber meshes due to the leave of GTP mlecules, which led to the release of DEX. In the following period, more H_2O molecules in PBS penetrated into the fiber matrix through these originally formed channels, and more DEX molecules were diffused out of the fiber meshes. Therefore, the enhancement of the release of DEX can be ascribed to the improvement of the

hydrophilicity of fiber matrix generated from the hydrophilicity of GTP.

Antibacterial Activity

One major issue for biomedical devices is the device-related bacterial infections and the resultant failure of treatment (37). Since GTP displays a good antibacterial property (38,39), we expected that the DEX-coentrapped GTP would also provide our new drug dressing with an antibacterial function. To assess this possible antibacterial capability, *E. Coli*, one of the predominat pathogenic bacteria for exogenous infection, were inoculated onto the petri dish; then the different formulated fiber meshs were loaded onto the surface of agar. As shown in Fig. 4, after 24 h incubation, lots of bacterial clonies were formed (Fig. 4a). When PLGA or PLGA/DEX fiber loaded, there was no obvious change, indicating that these two fiber meshes did not affect the bacterial growth (Fig. 4b & c). In contrast, a clear inhibition zone was formed for all of the bacterial dishes with GTP-loaded fiber meshes (Fig. 4d-f), indicating that the bactericidal effect of the fiber meshes may be attributed to GTP released from the fiber meshes. Moreover, the inhibition zone was gradually expanded along the loaded amout of GTP (average diameters of 11 ± 1.2, 14 ± 1.3 and 16 ± 1.2 mm, respectively), consistent with the GTP release kinetics (Fig. 3d), further suggesting a corresponding relationship between GTP content incorporated into the fiber mesh and the antibacterial effect obtained. Thus, the entrapped GTP renders the antibacterial property to DEX fiber mesh.

In Vitro Cytotoxicity Evaluation

To compare the biocompatibility of the drug-loaded fiber meshes with PLGA polymer, NIH 3 T3 fibroblasts were cultured onto the PLGA, DEX/PLGA, DEX/GTP5/PLGA, DEX/GTP10/PLGA, DEX/GTP15/PLGA fiber meshes for 7 days and cell viability was analyzed. As shown in Figure S3a, on the first day cell viability for all cultures on the meshes was more than 70% of the control cultures without the fiber meshed added. After 3 days, cell viability was obviously increased for all cultures. On day 5 & day 7, cell growth appeared to decline gradually except the culture on PLGA fiber meshes. Cells on the PLGA fiber meshes showed a better growing than the ones on the drug-loaded fiber meshes ($p < 0.05$). These results suggested that the loading of DEX caused a slight effect on biocompatibility of the PLGA fiber mesh, but the double drug loading did not further influence the biocompatibility. The reason may be owing to the good biocompatibility of GTP. We further observed the morphology of NIH-3 T3 fibroblasts grown on the fiber meshes with SEM. As shown in Figure S3b, the fibroblasts were attached and spreaded well on all fiber meshes. The SEM results matched well with the results of Alamar blue assay. From the analysis we can draw a conclusion that the introduction of GTP and DEX into fiber matrix almost did not influence the biocompatibility of PLGA polymer.

Since DEX was known to inhibit proliferation of the human keloid fibroblasts (hKFs) (20), cell growth of hKFs cultured on the fiber meshes with and without drug loading was then studied. The growth behavior of hKFs cultured in the

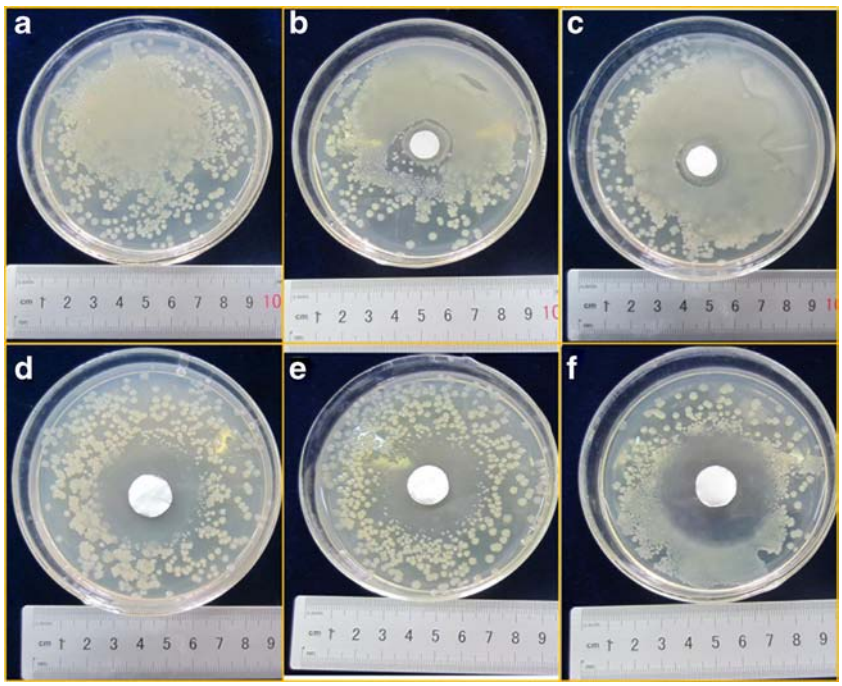

Fig. 4 Digital photographs of a Petri dish containing only *Escherichia coli.* as a comparison (**a**), the zones of inhibition of *Escherichia coli.* after a 24-h contact of PLGA fiber mesh (**b**) and DEX/PLGA (**c**), DEX/GTP5/PLGA (**d**), DEX/GTP10/PLGA (**e**) and DEX/GTP15/PLGAfiber meshes (**f**).

normal dish was firstly investigated. As shown in Figure S4a & b, after 1 week cultivation *in vitro*, cord-like cells started to gradually migrate out from the edge of the keloid tissue fragments. These fibroblasts exhibited a polygonal or long spindle shape, which was similar to normal fibroblast but larger. From the 2nd day to the 7th day these hKFs exhibited a significant increase in the proliferation rate; afterwards, the cells gradually went into a stationary growing phase, similarly to the prior report (40). DEX could cause the upregulation of VEGF in hKFs comparing to normal fibroblast, and the suppression of DEX on endogenous VEGF mRNA induction and protein expression of hKFs (20,21).

We then cultured the same hKFs onto the different formulated PLGA fiber meshes to determine cell viabilities of individual cultures. Fluorescence images were taken on Day 3 and Day 7 to visually display cells growing on the meshes. As expected, the electrospun meshes loaded with DEX alone significantly inhibited the growth of hKFs to some extent (Fig. 5a). Noticeably, all of the cultures on the DEX/GTP double-loaded meshes growed much slower than the culture on the DEX single-loaded one, particularly the Day 7 culture as shown, suggesting that co-entrapped of GTP would improve the inhibitory function of DEX to cell growth of hKFs. More interestingly, it was noticed that more GTP was loaded onto the meshes, a lower cell viability was obtained, showing a dose dependent intensifying effect of GTP on the inhibitory activity of DEX. Considering our early observation that the encapsulation of GTP promoted the release of hydrophobic DEX from PLGA fiber mesh (Fig. 3), we suggested that GTP may be able to modulate the inhibition of DEX to cell growth of hKFs. Figure 5b displays the survival and morphology of hKFs grown on the electrospun meshes and tissue culture

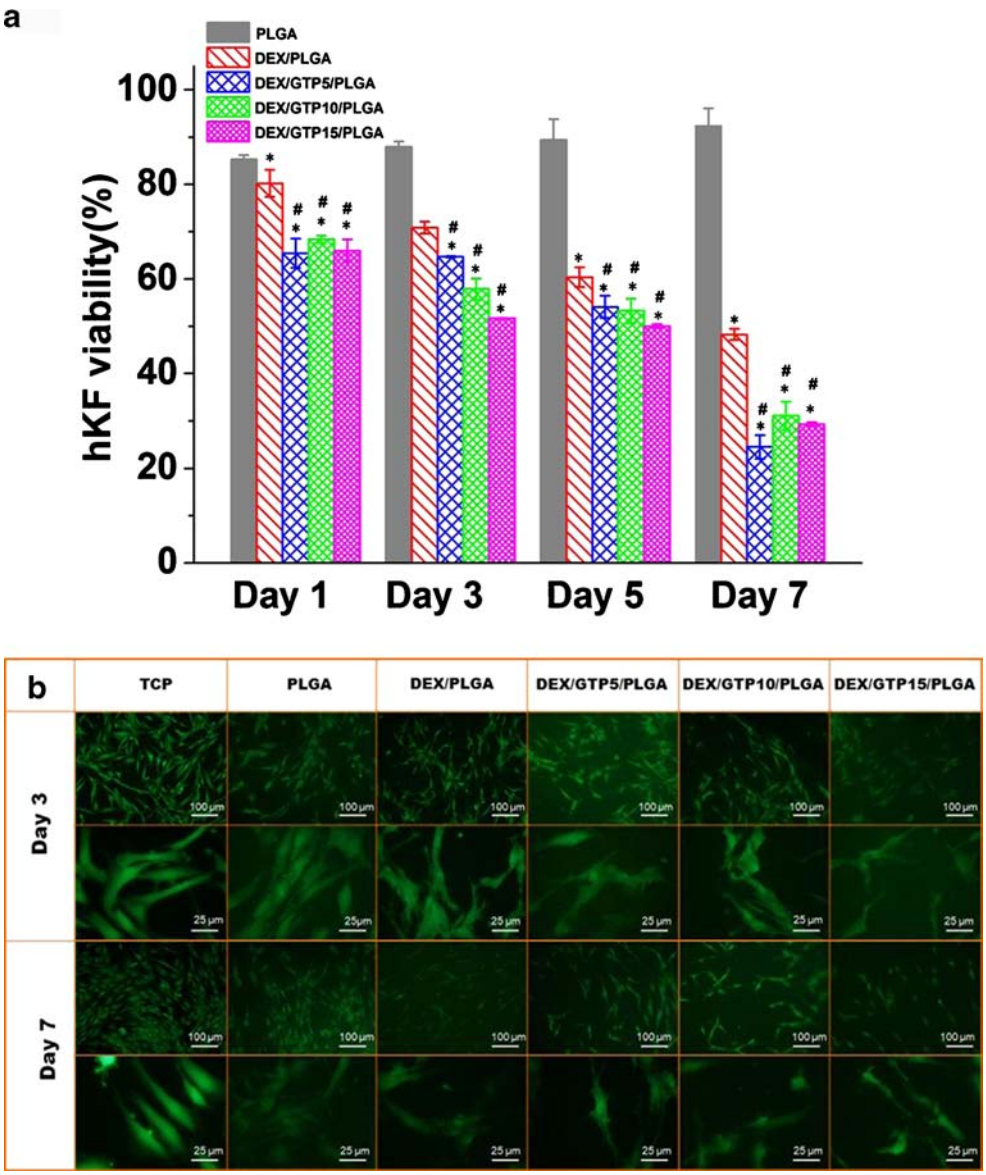

Fig. 5 (**a**) Human keloid fibroblasts (hKFs) cultured on electrospun fiber meshes; (**b**) fluorescence microscope images of human keloid fibroblasts (hKFs) cultured on electrospun fiber meshes for PLGA, DEX/PLGA, DEX/GTP5/PLGA, DEX/GTP10/PLGA, DEX/GTP15/PLGA. Cell survival and morphology was stained by Calcein AM for 3 and 7 days, and live cells appear as fluorescent *green color*. * indicates statistical difference from PLGA, and # indicates statistical difference from DEX/PLGA.

plates (TCP) on day 3 and day 7. When cultured on TCP and pure PLGA meshes, hKFs cells were spreading well and presenting a normal spindle-like or stellate shape without obvious branch. But when cultured on the drug-loaded electrospun meshes, hKFs were smaller, elongated and highly branched. More importantly, cells on all of the drug-loaded meshes became obviously less than the ones on TCP or PLGA meshes. These results further confirm that the DEX released from fiber meshes can suppress the growth of hKFs, and co-loading of GTP promotes this inhibition.

The Treatment Effect of Keloid Model in Nude Mice

To investigate the treatment effect of the drug-loaded PLGA fiber meshes *in vivo*, the human keloid tissues were subcutaneously implanted into the back of athymic nude mice as our keloid model (27). During 10 weeks of post-implantaton, keloids displayed a tendency to the normal distribution in their volume changes and reached a stable volume at the 8th week. And we did not observe any obvious skin ulcerations in the implanted sites (data not shown) (Figure S5). We then treated the implanted keloids (8 weeks) with the pure PLGA, DEX/PLGA, DEX/GTP10/PLGA meshes for 3 months to evaluate their restorative effects. Traditional silicon gel sheeting was used here as a control (Fig. 6a-d). During the whole animal experiment, any surgical incident was not found, suggesting that all mice tolerated the surgical procedure and the treatments were comfortable and safe. It is noticed that since in previous experiment the mice with the direct injection of DEX died in next day due to the strong side effects, we did not continue this experimental group in the following study. As shown in Fig. 6e, the treatment with silicon gel sheeting reduced the size of keloid obviously as expected, while PLGA fiber mesh alone did not cause significant decrease in volume of keloid. However, when DEX was loaded to PLGA electrospun fiber meshes, the keloids significantly shrinked (the keloid shrinkage volume of DEX/PLGA: 5.12 ± 0.48 mm^3 and DEX/GTP10/PLGA: 5.75 ± 0.39 mm^3) in contrast to ones treated with silicon gel sheeting (the keloid shrinkage volume of silicon gel sheeting: 4.01 ± 1.08 mm^3). Double loading of DEX and GTP into PLGA fiber meshes further decreased sizes of keloids. This result indicates that our drug-

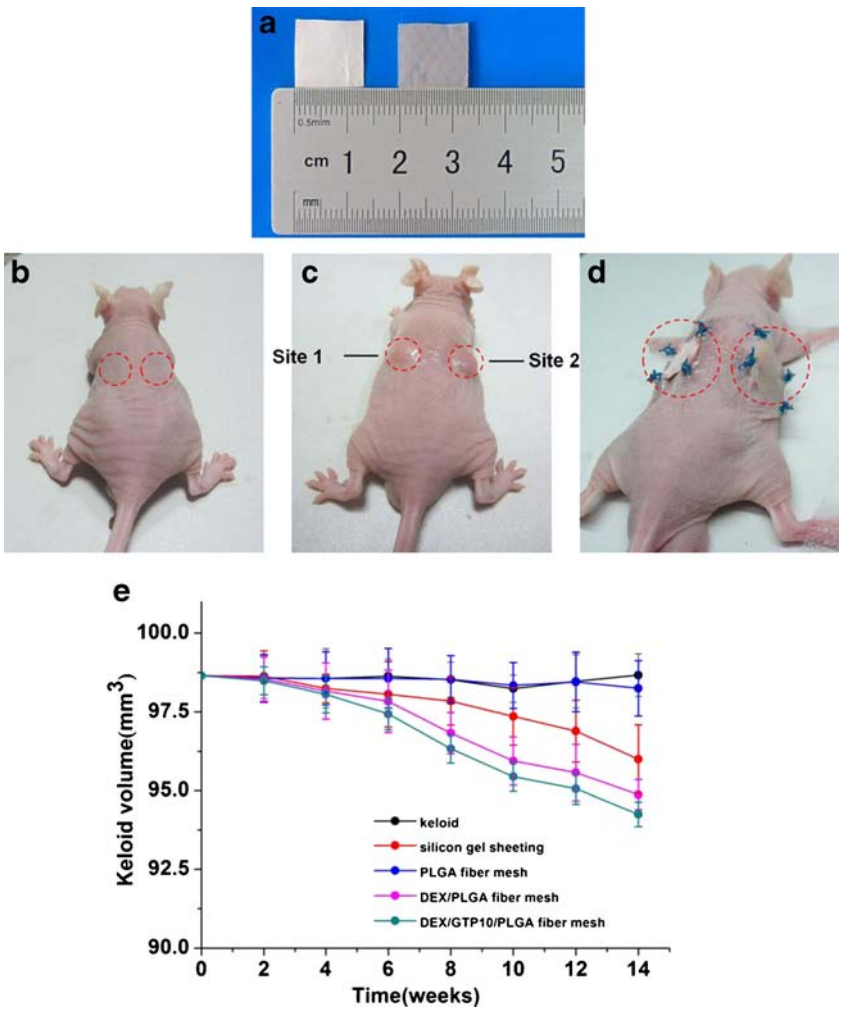

Fig. 6 (**a**) Fiber mesh and silicon gel sheeting were cut into small squares (1.3× 1.3 cm^2) and were wetted with saline before stuck to the keloid; (**b-d**) creation of keloid and treatment with fiber meshes. The *left* keloid (site 1) was fiber mesh and the *right* keloid (site 2) was used for silicon gel sheeting as control. (**e**) Volume change of the keloid treated with pure PLGA, DEX/PLGA, DEX/GTP10/PLGA fiber meshes and silicon gel sheeting for 3 months. Here, the untreated keloid as a control.

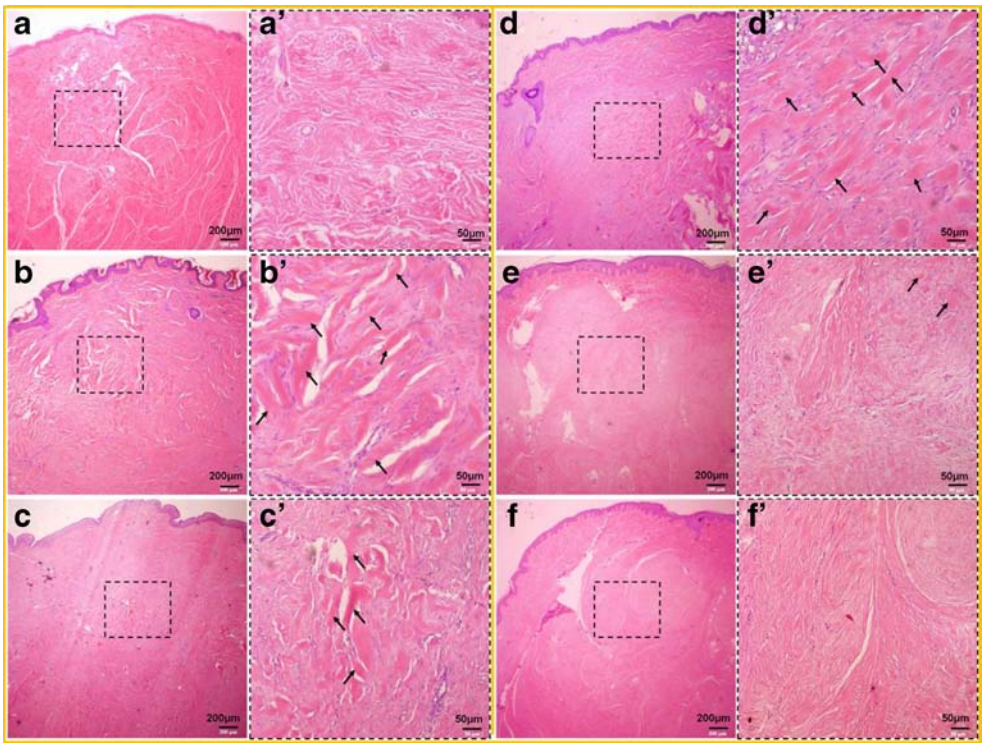

Fig. 7 H&E staining of normal skin (**a**), untreated keloid as a control (**b**), keloid biopsies from athymic nude mice covered with silicon gel sheeting (**c**), PLGA (**d**), DEX/PLGA (**e**), and DEX/GTP10/PLGA (**f**) fiber meshes after 3 months treatment. Magnified images in the black dotted squared area were displayed in the (**a′**, **b′**, **c′**, **d′**, **e′**, **f′**). Scale bars of the images with 40× and 200× magnification are 200 μm and 50 μm, respectively. The hyalinized collagen fibers were indicated wth *black arrows*.

loaded meshes can induce the regression of keloid *in vivo*, and the therapeutic effect is much better than silicon gel sheeting.

It was reported that the most distinct histologic characteristic of keloid is the presence of large, broad, closely arranged collagen fibers composed of numerous fibrils (41). To further assess the treatment effect of the fiber meshes on keloid, we harvested the keloid tissues from the mice treated with the fiber meshes and silicon gel sheeting for 3 months and then performed H&E staining (Fig. 7) and Masson's trichrome staining with them (Figure S6). As indicated by the black arrows in Fig. 7b, there were abundant collagen fibers in the dermis of untreated keloid with the nodular appearance, which was distinctively different from the normal skin structure with loosened collagen bundles as an ordered arrangement (Fig. 7a). Moreover, these collagen fibers were thick, hyalinized, and irregularly oriented and interspersed with haphazard arrangement fibroblasts. After treated with silicon gel sheeting, the keloid showed less amount of hyalinized collagen fibers, but the features of keloid were still remained as marked with black arrows in Fig. 7c. As expected, the treatment with pure PLGA mesh did not significantly change the histological structure of keloid (Fig. 7d). However, we observed that most of hyalinized collagen fibers were disappeared while the loose, thin and small collagen bundles appearing instead in the keloid after treated with DEX-loaded fiber meshes for 3 months (Fig. 7e), indicating that the treatment of DEX in electrospun fiber mesh is effective. In particular, no hyalinized collagen fibers were found after 3 months treatment with DEX/GTP-loaded fiber meshes (Fig. 7f). It also demonstrates that there is a significant improvement by GTP in therapeutic effect of DEX on keloid accompanied with the disappearance of the distinguishing characteristic of keloid. The result may be due to the released DEX facilitated by the hydrophilic GTP and the antibacterial activity endowed by the introduction of GTP. In addition, Masson's staining also displayed a consistent reduction in collagen fibers after treated with DEX/GTP-loaded fiber meshes as shown in Figure S6. It further demonstrates that the dual drug-loaded fiber meshes are very effective in restoring the keloid to normal skin tissue *in vivo*.

CONCLUSIONS

In summary, the electrospun PLGA fiber meshes were successfully fabricated for co-delivering of DEX and GTP, which were applied as a dressing formulation for transdermal drug delivery. Through the introduction of hydrophilic GTP into PLGA fiber meshes, these fiber meshes possessed versatile functions including the capabilities of maintaining a moist environment, resisting bacterial infection, and controlling the drug release. *In vitro* cytotoxicity analysis revealed that DEX/GTP-loaded fiber meshes had a good biocompatibility through co-culture with NIH-3 T3 normal fibroblasts, and a high suppression for human keloid fibroblasts. Compared with traditional treatment with silicon gel sheeting, the dual

drug-loaded fiber meshes represented a more significant improvement in therapeutic effect with the disappearance of the distinguishing characteristic of keloid in nude mice after 3 months treatment. The dress formulation acquires a good balance between the effective treament of keloid and safety to the skin.

ACKNOWLEDGMENTS AND DISCLOSURES

Jinrong Li and Rong Fu are co-first authors. This work was partially supported by National Basic Research Program of China (973 Program, 2012CB933600), National Natural Science Foundation of China (No.30970723 and No.51173150), National Key Project of Scientific and Technical Supporting Programs Funded by MSTC (2012BAI17B06), Key Project in the Science and Technology Pillar Program from Sichuan Science and Technology Bureau (2102SZ0076) and Fundamental Research Funds for The Central Universities (SWJTU11ZT10). We are grateful to Prof. X.D. Li in Sichuan University for kindly providing GTP, and to Prof. Y.P. Chen for valuable discussion.

REFERENCES

1. Singer AJ, Clark RA. Cutaneous wound healing. N Engl J Med. 1999;341(10):738–46.
2. Gurtner GC, Werner S, Barrandon Y, Longaker MT. Wound repair and regeneration. Nature. 2008;453(7193):314–21.
3. Atiyeh BS, Costagliola M, Hayek SN. Keloid or hypertrophic scar: the controversy: review of the literature. Ann Plast Surg. 2005;54(6): 676–80.
4. Alster TS, Williams CM. Treatment of keloid sternotomy scars with 585 nm flashlamp-pumped pulsed-dye laser. Lancet. 1995;345(8959):1198–200.
5. Butler PD, Longaker MT, Yang GP. Current progress in keloid research and treatment. J Am Coll Surg. 2008;206(4):731–41.
6. Lutgendorf MA, Adriano EM, Taylor BJ. Prevention and management of keloid scars. Obstet Gynecol. 2011;118(2):351–6.
7. Schacke H, Docke WD, Asadullah K. Mechanisms involved in the side effects of glucocorticoids. Pharmacol Ther. 2002;96(1):23–43.
8. Reish RG, Eriksson E. Scar treatments: preclinical and clinical studies. J Am Coll Surg. 2008;206(4):719–30.
9. O'Brien L, Pandit A. Silicon gel sheeting for preventing and treating hypertrophic and keloid scars. Cochrane Database Syst Rev. 2006;1: 1–32.
10. Prausnitz MR, Langer R. Transdermal drug delivery. Nat Biotechnol. 2008;26(11):1261–8.
11. Huang C, Lucas B, Vervaet C, Braeckmans K, Van Calenbergh S, Karalic I, *et al.* Unbreakable codes in electrospun fibers: digitally encoded polymers to stop medicine counterfeiting. Adv Mater. 2010;22(24):2657–62.
12. Sofokleous P, Stride E, Edirisinghe M. Preparation, Characterization, and Release of Amoxicillin from Electrospun Fibrous Wound Dressing Patches. Pharmaceut Res. 2013;30(7): 1926–38.
13. Dong B, Smith ME, Wnek GE. Encapsulation of multiple biological compounds within a single electrospun fiber. Small. 2009;5(13): 1508–12.
14. Bashur CA, Dahlgren LA, Goldstein AS. Effect of fiber diameter and orientation on fibroblast morphology and proliferation on electrospun poly(D, L-lactic-co-glycolic acid) meshes. Biomaterials. 2006;27(33):5681–8.
15. Bhardwaj N, Kundu SC. Electrospinning: A fascinating fiber fabrication technique. Biotechnol Adv. 2010;28(3):325–47.
16. Ji W, Sun Y, Yang F, van den Beucken J, Fan M, Chen Z, *et al.* Bioactive electrospun scaffolds delivering growth factors and genes for tissue engineering applications. Pharmaceut Res. 2011;28(6): 1259–72.
17. MacNeil S. Progress and opportunities for tissue-engineered skin. Nature. 2007;445(7130):874–80.
18. Rho KS, Jeong L, Lee G, Seo BM, Park YJ, Hong SD, *et al.* Electrospinning of collagen nanofibers: effects on the behavior of normal human keratinocytes and early-stage wound healing. Biomaterials. 2006;27(8):1452–61.
19. Lalani R, Liu LY. Electrospun zwitterionic poly(sulfobetaine methacrylate) for nonadherent, superabsorbent, and antimicrobial wound dressing applications. Biomacromolecules. 2012;13(6): 1853–63.
20. Wu WS, Wang FS, Yang KD, Huang CC, Kuo YR. Dexamethasone induction of keloid regression through effective suppression of VEGF expression and keloid fibroblast proliferation. J Invest Dermatol. 2006;126(6):1264–71.
21. Lamy S, Gingras D, Beliveau R. Green tea catechins inhibit vascular endothelial growth factor receptor phosphorylation. Cancer Res. 2002;62(2):381–5.
22. Hamilton-Miller JM. Antimicrobial properties of tea (Camellia sinensis L.). Antimicrob Agents Chemother. 1995;39(11):2375–7.
23. Gordon NC, Wareham DW. Antimicrobial activity of the green tea polyphenol (-)-epigallocatechin-3-gallate (EGCG) against clinical isolates of Stenotrophomonas maltophilia. Int J Antimicrob Agents. 2010;36(2):129–31.
24. Zhou SB, Deng XM, Yang H. Biodegradable poly(ε-caprolactone)-poly(ethylene glycol) block copolymers: characterization and their use as drug carriers for a controlled delivery system. Biomaterials. 2003;24(20):3563–70.
25. Luo C, Li L, Li J, Yang G, Ding S, Zhi W, *et al.* Modulating cellular behaviors through surface nanoroughness. J Mater Chem. 2012;22(31):15654–64.
26. Shao SJ, Zhou SB, Li L, Li J, Luo C, Wang J, *et al.* Osteoblast function on electrically conductive electrospun PLA/MWCNTs nanofibers. Biomaterials. 2011;32(11):2821–33.
27. Shetlar MR, Shetlar CL, Hendricks L, Kischer CW. The Use of Athymic Nude Mice for the Study of Human Keloids. Experimental Biology and Medicine. 1985;179(4):549–52.
28. Chen T, Guo X, Liu X, Shi S, Wang J, Shi C, *et al.* A strategy in the design of micellar shape for cancer therapy. Adv Healthc Mater. 2012;1(2):214–24.
29. Jayakumar R, Prabaharan M, Sudheesh Kumar PT, Nair SV, Tamura H. Biomaterials based on chitin and chitosan in wound dressing applications. Biotechnol Adv. 2011;29(3): 322–37.
30. Chew SY, Hufnagel TC, Lim CT, Leong KW. Mechanical properties of single electrospun drug-encapsulated nanofibres. Nanotechnology. 2006;17(15):3880–91.
31. Blasi P, D'Souza SS, Selmin F, DeLuca PP. Plasticizing effect of water on poly(lactide-co-glycolide). J Control Release. 2005;108(1): 1–9.
32. Ma K, Yong T, Chan KC, Ramakrishna S. Collagen-blended biodegradable polymer nanofibers: potential substrates for wound healing in skin tissue engineering. Proc Fifth IASTED Inter Conf Biomed Eng ACTA Press Anaheim CA 2007:262–266.
33. Dong YX, Liao SS, Ngiam M, Chan CK, Ramakrishna S. Degradation behaviors of electrospun resorbable polyester nanofibers. Tissue Eng Part B Rev. 2009;15(3):333–51.

34. Deng XM, Zhou SB, Li X, Zhao J, Yuan M. *In vitro* degradation and release profiles for poly-dl-lactide-poly(ethylene glycol) microspheres containing human serum albumin. J Control Release. 2001;71(2):165–73.
35. Luong-Van E, Grøndahl L, Chua KN, Leong KW, Nurcombe V, Cool SM. Controlled release of heparin from poly(ε-caprolactone) electrospun fibers. Biomaterials. 2006;27(9):2042–50.
36. Szentivanyi A, Chakradeo T, Zernetsch H, Glasmacher B. Electrospun cellular microenvironments: understanding controlled release and scaffold structure. Adv Drug Deliver Rev. 2011;63(4–5):209–20.
37. Vasilev K, Cook J, Griesser HJ. Antibacterial surfaces for biomedical devices. Expert Rev Med Devices. 2009;6(5):553–67.
38. Friedman M. Overview of antibacterial, antitoxin, antiviral, and antifungal activities of tea flavonoids and teas. Mol Nutr Food Res. 2007;51(1):116–34.
39. Sharma A, Gupta S, Sarethy IP, Dang S, Gabrani R. Green tea extract: possible mechanism and antibacterial activity on skin pathogens. Food Chem. 2012;135(2):672–5.
40. Giugliano G, Pasquali D, Notaro A, Brongo S, Nicoletti G, D'Andrea F, *et al.* Verapamil inhibits interleukin-6 and vascular endothelial growth factor production in primary cultures of keloid fibroblasts. Br J Plast Surg. 2003;56(8):804–9.
41. Sidle DM, Kim H. Keloids: prevention and management. Facial Plast Surg Clin North Am. 2011;19(3):505–15.